Transcriptional bursting diversifies the behaviour of a toggle switch: hybrid simulation of stochastic gene expression

Pavol Bokes [1,⋆], John R. King [2], Andrew T. A. Wood [2], Matthew Loose [3]

[1] *Department of Applied Mathematics and Statistics, Comenius University, Mlynská dolina, Bratislava 842 48, Slovakia*

[2] *Centre for Mathematical Medicine and Biology, School of Mathematical Sciences, University of Nottingham, Nottingham NG7 2RD, UK*

[3] *Institute of Genetics, Queen's Medical Centre, University of Nottingham, Nottingham NG7 2UH, UK*

[⋆] *E-mail:* pavol.bokes@fmph.uniba.sk

Abstract

Hybrid models for gene expression combine stochastic and deterministic representations of the underlying biophysical mechanisms. According to one of the simplest hybrid formalisms, protein molecules are produced in randomly occurring bursts of a randomly distributed size while they are degraded deterministically. Here we use this particular formalism to study two key regulatory motifs — the autoregulation loop and the toggle switch. The distribution of burst times is determined and used as a basis for the development of exact simulation algorithms for gene expression dynamics. For the autoregulation loop, the simulations are compared to an analytic solution of a master equation. Simulations of the toggle switch reveal a number of qualitatively distinct scenarios with implications for the modelling of cell-fate selection.

1 Introduction

The typical abundances of the various biochemical species involved in the regulation of gene expression range from very few to many thousands [1, 2]. Genes are typically present at low copy numbers, while proteins can be highly abundant [1]; mRNA transcripts are scarce in prokaryotic cells [2], but they can be copious in eukaryotes [3]. The mechanisms affecting only the abundant species (translation, protein decay, eukaryotic transcription and mRNA decay) will consequently be largely deterministic, while those

involving scarce species (promoter transitions, prokaryotic transcription and mRNA decay) will be stochastic.

Mathematical models that consist of stochastic jump processes with deterministic behaviour between jumps are called piecewise deterministic processes [4] or stochastic hybrid models [5]. Hybrid modelling facilitated the analysis of a range of biological phenomena, such as the dynamics of cell dispersal [6], the self-assembly of microtubules [7], spontaneous neuronal action potentials [8], as well as stochastic gene expression [5]. Hybrid models for gene expression typically concern a single gene copy, whose promoter randomly transitions between an active and an inactive state like a random telegraph [9–12]. The levels of the mRNA and protein encoded by the gene are treated as continuous quantities, which obey ordinary differential equations. Stochasticity generated at the promoter stage is transmitted down to the mRNA and protein levels by assuming that the transcription rate depends on the promoter activity state. Transcriptional regulation can be modelled by assuming that the stochastic rates of promoter activation and/or inactivation depend on the protein level [13].

There are a number of variations on the above formalism. First, some species, such as mRNA molecules, may be treated as continuous (abundant) in some models and as discrete (scarce) in others [5]. Second, jumps may occur either at random times or at regularly spaced time points. Stochastic jump processes that are discrete not only in state space but also in time have been used as part of a hybrid model for a regulatory cascade governing subtilin production in *B. subtilis* [14]. Third, the deterministic mechanisms can be extended by diffusion noise [15–17]. These three examples illustrate the variety of modelling approaches available when using the hybrid formalism.

The hybrid model studied in [9–12] (stochastic promoter, deterministic mRNA and protein) reduces into a particularly important special case if the promoter is inactive for most of the time, with the exception of short periods of rapid transcription [18]. The length of any such period is exponentially distributed if one considers the simplest possible inactivation mechanism — a single memoryless random step [18]. The amount of mRNA transcribed is proportional to the length of the period and is therefore exponentially distributed too [19]. If the two processes are fast, the production of the exponentially distributed amount of transcript virtually occurs as a single event, and this is referred to as a burst; the amount of transcript produced in a burst is the burst size [18].

Neglecting any delay resulting from the elongation and translation processes, a burst of mRNAs spurs an immediate burst of protein synthesis. The size of the protein burst is proportional to that of mRNA, the factor of proportionality being given by the balance between the rates of translation and mRNA decay [20].

Proteins are degraded, and the decay process is deterministic provided that they are abundant [19]. The balance between the protein synthesis in exponential bursts occurring at random times and the deterministic decay gives the overall hybrid protein dynamics on which we shall focus in this paper. The main advantage of this model is its simplicity: neither promoter state nor mRNA level is explicitly present in it; at the same time it is physically well justified. It was originally used to describe translational bursting in prokaryotes [19]. Its relationship to other descriptions of bursting gene expression has been characterised using singular-perturbation and system-size expansions in [17].

In this paper we use the hybrid formalism for burst-like protein dynamics to study two key regulatory motifs, the autoregulation loop [21, 22] and the toggle switch [23] (see also e.g. [24–29], which are reviewed in more detail at a later point in this paper). For both motifs the distribution of burst times is characterised, and algorithms for exact stochastic simulations are presented. The simulations of the autoregulation loop are compared to an analytic solution to the master equation. For the toggle switch we report that bistability and co-expression scenarios of the deterministic model [23] each have their counterparts in the hybrid stochastic formulation, but that these can further be divided into qualitatively distinct sub-categories depending on the level of gene-expression noise present. The various possible types of behaviour are interpreted in the context of a developmental switch that governs cell-fate selection.

2 Autoregulation

We consider a stochastic model for gene expression dynamics, in which a transcription factor X (TF X) is degraded deterministically with rate constant γ, but its transcription is stochastic, occurring in discrete events [19]. The transcription rate may depend on the current level x of X (measured in arbitrary units); various choices can be made regarding its functional form, $a(x)$, one of the most common being the S-shaped function [30–32]

$$a(x) = a_0 + \frac{a_1 K^n}{K^n + x^n}. \tag{1}$$

Here $a_0 > 0$ is the minimal, or basal, transcription rate. The parameter $a_1 > 0$ gives the difference between the minimal and maximal rates. The dissociation constant $K > 0$ gives the amount of X that sets the transcription rate to the arithmetic average of the minimal and maximal rates. The Hill constant n can be positive or negative, with $n > 0$ corresponding to negative feedback and $n < 0$ corresponding to positive feedback [*].

Each transcription event leads to a production of a quantity of X. The event is referred to as transcription burst and the quantity produced is the size of the burst.

[*] Alternatively, $n > 0$ could be required in place of $a_1 > 0$, with $a_1 < 0$ corresponding to positive feedback.

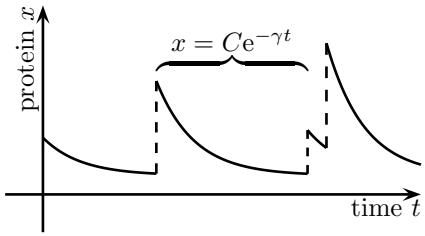

Figure 1: Hybrid protein expression dynamics.

Each burst size is assumed to be statistically independent of the past protein dynamics and distributed exponentially with some specific mean b (refer back to Section 1 for a justification). A typical temporal dynamics of x is shown in Figure 1.

Below, we review the previous analysis [19] of the associated master equation (Section 2.1) and the main properties of its deterministic reduction (Section 2.2). The probabilistic properties of burst timing are examined in Section 2.3, the results of which facilitate the stochastic simulation of the hybrid autoregulation model (Section 2.4).

2.1 The master equation

The probability $p(x,t)$ of observing an amount x of X per unit margin satisfies the master equation [19]

$$\frac{\partial p}{\partial t} - \gamma \frac{\partial (xp)}{\partial x} = w * (ap), \tag{2}$$

where $*$ is the convolution operation with respect to $x \geq 0$ and

$$w(x) = \frac{\mathrm{e}^{-x/b}}{b} - \delta(x) \tag{3}$$

is the burst kernel (the integral of w over $x \geq 0$ is required to be zero to conserve total probability). In other words, the right-hand side of (2), when evaluated at specific values x and t, is given by

$$w * (ap)(x,t) = \int_0^x w(x-z)a(z)p(z,t)\mathrm{d}z = \frac{1}{b}\int_0^x \mathrm{e}^{-(x-z)/b}a(z)p(z,t)\mathrm{d}z - a(x)p(x,t).$$

If $a \equiv 0$, i.e. in the absence of any transcription, the right-hand side of (2) is zero and the integro-differential equation reduces to the continuity equation corresponding to linear decay $\mathrm{d}x/\mathrm{d}t = -\gamma x$. If $a \not\equiv 0$, then $a(x)p(x,t)$ gives the part of the density that is subject to transcription per unit time; by convolving $a(x)p(x,t)$ with the kernel $w(x)$, we obtain what the density transforms into after a transcriptional burst. Superimposing the convolution term on the continuity equation gives the complete dynamics (2).

From now on we assume that $\gamma = 1$ and $b = 1$, as this can always be achieved by measuring time in the units of the TF lifetime $1/\gamma$ and measuring abundance in the units of the mean burst size b.

For constitutive promoter, i.e. if $a(x) \equiv a$ is a constant with respect to x, equation (2) is satisfied by the gamma distribution, see [19],

$$p(x) = \frac{1}{\Gamma(a)} \mathrm{e}^{-x} x^{a-1}, \quad \text{if } a(x) \equiv a. \tag{4}$$

For the S-shaped functional form (1) of the transcription rate $a(x)$, the normalised stationary solution of (2) is given, see [19], by

$$p(x) = C \mathrm{e}^{-x} x^{a_0+a_1-1} (K^n + x^n)^{-a_1/n}, \tag{5}$$

where C is the normalisation constant. The conditions for (5) to be bimodal have been compared to the conditions for the deterministic reduction of (2), see below, to be bistable [33]. Global stability of the stationary solution (5) to (2) was established using semigroup theory in [34], see also [33]. Interestingly, the distribution (5) can also be obtained from a very different autoregulation model, according to which protein synthesis is deterministic and all the noise is due to a stochastic drift-diffusion decay [33].

2.2 The deterministic reduction

Multiplying the master equation (2) by x and then integrating it with respect to x ranging from zero to infinity, we find that

$$\frac{\mathrm{d}\langle x \rangle}{\mathrm{d}t} = -\gamma \langle x \rangle + b \langle a(x) \rangle, \tag{6}$$

where $\langle \cdot \rangle$ denotes the expected value.

The deterministic reduction of (2) is obtained by neglecting fluctuations in (6), see [35], which yields

$$\frac{\mathrm{d}x}{\mathrm{d}t} = -\gamma x + b \cdot a(x) = -\gamma x + c_0 + \frac{c_1 K^n}{K^n + x^n}, \tag{7}$$

where $c_0 = b \cdot a_0$ gives the amount of protein synthesised per unit time under total repression and $c_1 = b \cdot a_1$ is the amount per unit time by which the production can be boosted by autoregulation.

The nonlinear first-order ordinary differential equation (7) is one of the most basic deterministic models for transcriptional autoregulation [21, 22]. If the autoregulation is positive and cooperative, i.e. if $n < -1$, then (7) exhibits hysteresis and, depending on the parameter values, can possess up to two stable steady states [30]. If $n \geq -1$, then equation (7) possesses a unique stable steady state. In the case of highly cooperative negative autoregulation, i.e. for n positive and large, the level of the stable steady state is typically close to the dissociation constant K and is insensitive to variations in the remaining parameters [36]. The positive autoregulation loop enables the living cell

to "remember" past occurrences [30], while the negative autoregulation loop makes a homeostatic response to changing external stimuli possible [36]. The negative loop can drive biological oscillations if the model is extended by a suitable delay mechanism [37].

2.3 Burst times

Suppose that at the initial time $t = 0$ we know the level x of X, and we want to characterise the waiting time T until the next burst occurs. The random variable T (for a fixed x) can be described by its hazard function (or hazard rate) $h(t) \geq 0$, which is defined by the relationship, cf. [38],

$$P[T \leq t + \mathrm{d}t | T > t] = h(t)\mathrm{d}t + o(\mathrm{d}t), \tag{8}$$

this being equivalent to stating, cf. [38],

$$P[T > t] = \exp\left(-\int_0^t h(\tau)\mathrm{d}\tau\right)$$

for the distribution of T.

The hazard function of the burst time T can easily be expressed in terms of the transcription rate $a(x)$. The condition $T > t$ in (8) implies that no bursts occurred between the initial time and time t, during which X decays with unit rate constant, its level falling to $x\mathrm{e}^{-t}$ at time t. Consequently,

$$h(t) = a(x\mathrm{e}^{-t}) = a_0 + \frac{a_1 K^n}{K^n + x^n \mathrm{e}^{-nt}}.$$

We partition the hazard function into a sum of two,

$$h(t) = h_0(t) + h_1(t),$$

where

$$h_0(t) = a_0, \quad h_1(t) = \frac{a_1 K^n}{K^n + x^n \mathrm{e}^{-nt}},$$

identifying $h_0(t)$ with the constant hazard of a basal transcription burst and $h_1(t)$ with the hazard of a regulated transcription burst.

The timing of the next burst can be determined using the following general result [38]:

Lemma 1 *If T_0 and T_1 are independent waiting times with hazard functions $h_0(t)$ and $h_1(t)$, then $T = \min(T_0, T_1)$ has hazard function $h(t) = h_0(t) + h_1(t)$.*

A waiting time T_0 with hazard function $h_0(t) \equiv a_0$ is exponentially distributed with mean equal to the reciprocal $1/a_0$ of the rate [38]. We interpret the variable T_0 as the

candidate waiting time for basal transcription. By the inversion sampling method [39], a realisation t_0 of T_0 can be drawn by setting

$$t_0 = -\frac{\ln u_0}{a_0}, \tag{9}$$

where u_0 is a random variate drawn from the standardised uniform distribution.

The cumulative distribution function of a waiting time T_1 with hazard function $h_1(t)$ satisfies

$$P[T_1 > t] = \exp\left(-\int_0^t h_1(\tau)\mathrm{d}\tau\right) = \left(\frac{x^n + K^n}{x^n + K^n \mathrm{e}^{nt}}\right)^{\frac{a_1}{n}}. \tag{10}$$

The variable T_1 can be interpreted as the candidate waiting time for a regulated burst: it is not the real waiting time, because a number of basal bursts may precede, and change the hazard rate of, the regulated transcription burst we are waiting for.

By the inversion sampling method, we can draw a realisation t_1 of T_1 by equating (10) to a uniformly distributed random variate $0 < u_1 < 1$, solving the resultant equation in t, and taking for t_1 the (unique) solution if it exists, or setting $t_1 = \infty$ if it does not; this yields

$$t_1 = \begin{cases} \dfrac{1}{n}\ln\left(u_1^{-\frac{n}{a_1}}(1 + (x/K)^n) - (x/K)^n\right) & \text{if } u_1^{\frac{n}{a_1}} < 1 + (K/x)^n, \\ \infty & \text{otherwise.} \end{cases} \tag{11}$$

While for $n > 0$ the candidate waiting time T_1 is always finite, for $n < 0$ it is infinite with probability $(1+(K/x)^n)^{\frac{a_1}{n}}$ (this can be established either from (11) or directly from (10) by taking $t \to \infty$). Recalling that negative n corresponds to positive autoregulation, infinite T_1 pertains to the possibility that the TF decays to low levels at which it can no longer sustain transcription.

In view of Lemma 1, we draw a realisation t of the waiting time T for the next transcription burst by setting

$$t = \min(t_0, t_1), \tag{12}$$

where t_0 and t_1 are defined by (9) and (11), whereby u_0 and u_1 are independently drawn from the standardised uniform distribution.

Between the initial time and the burst time t given by (12) the level of X decays with unit rate constant, so that $x\mathrm{e}^{-t}$ gives the level of X just before the burst occurs. The size of the burst is exponentially distributed with mean equal to unit abundance and independent of the past dynamics of X. Therefore, by the inversion sampling method, the level $\tilde{x}$ of X just after the burst can be determined by

$$\tilde{x} = x\mathrm{e}^{-t} - \ln\tilde{u},$$

where $\tilde{u}$ is drawn from the standardised uniform distribution independently of u_0 and u_1. Hence, having started at the initial time zero with a given level x, we are able to

Require: An initial distribution $X^{(0)} \geq 0$ and a parameter set (a_0, a_1, n, K).

Return: A sample trajectory $x(t)$, $t \geq 0$, of TF expression dynamics.

Draw the initial state $x^{(0)}$ from the initial distribution $X^{(0)}$.
Set the current time and state: $t \leftarrow 0$; $x(0) \leftarrow x^{(0)}$.
loop
    Draw three independent variates u_0, u_1 and $\tilde{u}$ from the standardised uniform distribution.
    if $a_0 > 0$ **then**
        Set $\tau_0 \leftarrow -\frac{\ln u_0}{a_0}$.
    else
        Set $\tau_0 \leftarrow \infty$.
    end if
    if $u_1^{\frac{n}{a_1}} < 1 + (K/x(t))^n$ **then**
        Set $\tau_1 \leftarrow \frac{1}{n}\ln\left(u_1^{-\frac{n}{a_1}}(1 + (x(t)/K)^n) - (x(t)/K)^n\right)$.
    else
        Set $\tau_1 \leftarrow \infty$.
    end if
    Set $\tau \leftarrow \min\{\tau_0, \tau_1\}$.
    Set $x(t + \delta) \leftarrow x(t)\mathrm{e}^{-\delta}$ for $0 < \delta < \tau$.
    Set $x(t + \tau) \leftarrow x(t)\mathrm{e}^{-\tau} - \ln(\tilde{u})$.
    Update the current time $t \leftarrow t + \tau$.
end loop

Algorithm 1: Hybrid simulation of autoregulation

sample the TF dynamics for the next t units of time, ending up with the level $\tilde{x}$. We may then start afresh from time t and level $\tilde{x}$ and prosecute the whole procedure over again to sample the dynamics until the second burst, and then again until the third occurs, etc., until we have sampled the dynamics over a period of our choosing. The boundedness of the transcription rate $a(x)$ ensures that the sequence of burst times will with probability one converge to infinity and the TF dynamics cannot "blow up" in finite time. The pseudocode for hybrid simulation of autoregulation dynamics is given in full as Algorithm 1 (note that in it we use τ_0, τ_1 and τ for waiting times and t for the total cumulative time).

2.4 Simulations

We introduce the logarithmic scale

$$x = 10^y.$$

The decimal base is chosen because it is more convenient for visualisation purposes than the mathematically appealing natural base. The density $q(y)$ of y is obtained from the density $p(x)$ of x by the transformation rule

$$q(y) = p(10^y)\frac{\mathrm{d}(10^y)}{\mathrm{d}y} = p(10^y)10^y \ln(10).$$

Using (5), we find that the log-scaled level of a self-regulating TF is distributed with density

$$q(y) = \tilde{C}\exp(-10^y)10^{(a_0+a_1)y}(K^n + 10^{ny})^{-\frac{a_1}{n}}, \tag{13}$$

where $\tilde{C}$ is the normalisation constant. The use of the logarithmic scale eliminates the singularity at $x = 0$ of the original density (5) which occurs if $a_0 + a_1 < 1$ (for $n > 0$) or if $a_0 < 1$ (for $n < 0$); the boundedness of the transformed density (13) will facilitate its visualization.

We examine a specific parameter set characterised by an infrequent leakage ($a_0 = 0.5$), which can be up-regulated to up to 5 bursts per protein lifetime ($a_1 = 4.5$) via a sharp positive autoregulation loop ($K = 2$, $n = -6$). Given these values, the deterministic model (16) possesses two stable steady states, a basal expression state ($x_{\mathrm{low}} \approx 0.501$), and an up-regulated state ($x_{\mathrm{high}} \approx 4.98$). Below, we investigate the behaviour of the hybrid model in this regime (see [40] for further simulations).

We implemented Algorithm 1 in a suitable high-level programming language (our choice is Python enhanced by the packages NumPy, SciPy and Matplotlib) and generated a large number $N = 20000$ of mutually independent trajectories $x_i(t)$, $i = 1, \ldots, N$, of the TF dynamics for the given parameter set ($a_0 = 0.5$, $a_1 = 4.5$, $K = 2$ and $n = -6$)

and subject to the initial condition $X^{(0)} = 10^{Y^{(0)}}$, where $Y^{(0)}$ is the standardised normal distribution.

The logarithmically transformed trajectories $y_i(t) = \log_{10}(x_i(t))$, $i = 1, \ldots, N$, provide us, for any fixed value of time t, with the dataset $\{y_i(t)\}_{i=1}^N$. These large datasets contain enough information for non-parametric estimation of the distribution of the underlying process. Figures 2Ai–iv show histograms $\hat{q}(y, t)$ based on the datasets $\{y_i(t)\}_{i=1}^N$ for selected values of time t and compare these histograms to the theoretical stationary distribution $q(y)$: we can see that as time increases, the histograms converge to the stationary distribution. The stationary distribution is bimodal, the two modes corresponding to the basal and up-regulated states of protein dynamics.

Figures 2Bi–iv show the histogram evolution for the same choice of parameters but with a different initial distribution: we consider one that has the whole probability mass concentrated around the lower of the two modes of the stationary distribution so as to observe the dynamics of the transfer of the mass to the other mode. Specifically, we choose the gamma distribution with the shape parameter a_0, which gives the stationary expression of a protein which is transcribed at the constant basal rate $a(x) \equiv a_0$, cf. equation (4). Biologically, this choice of initial distribution indicates that, prior to the initial time $t = 0$, the autoregulatory loop of X was disabled (say X was modified by an interaction with signalling molecules that prevented it from binding to the DNA); the expression of X stabilised at a basal level. At $t = 0$ the autoregulatory interaction is established (say the signalling that previously disrupted DNA binding is switched off), and we observe the evolution of the basal level to a bi-modal expression.

In Figures 2Ci–iv, we use the gamma distribution with shape parameter $a_0 + a_1$, this being the stationary distribution for a protein transcribed constitutively at the maximal transcription rate $a_0 + a_1$. Again, such an initial state models a biologically relevant situation, in some respect complementary to the previous one. In transcriptional regulation X binds to the gene promoter, catalysing (if we are concerned with positive autoregulation) the initiation of transcription. The binding to the promoter can be unspecific, and a different transcription factor with a similar chemical structure, say T, may substitute for X to the same effect. Assume that T is constitutively expressed, and highly abundant, but is activated only in the presence of a certain signal. If prior to $t = 0$ the signalling is present, the abundant substitute T saturates the binding site, leading to the maximal expression rate of $a_0 + a_1$ (Figure 2Ci). If the signal is switched off at $t = 0$, the TF X takes over the regulation and sustains its own expression via a positive feedback (Figures 2Cii–iv).

Note that the convergence of the histograms of the generated data to the stationary distribution as time t increases is faster if the probabilistic mass of the initial distribution

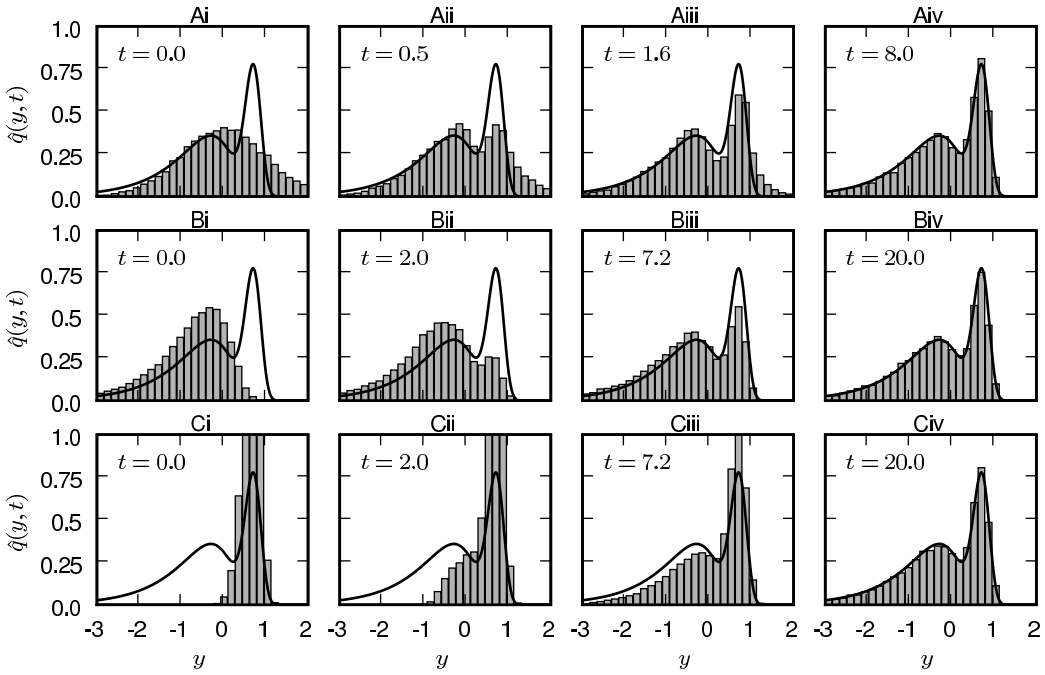

Figure 2: The histograms of the log-scaled expression levels of X, generated by the algorithm for the positive autoregulation process (Algorithm 1), approach as time t increases the theoretical stationary probability density function (the solid line), which is given by (13). The parameters of the process and the probability law of the three specific initial conditions considered (corresponding to the histograms in Figures 2Ai, Bi and Ci) are detailed in the main text. Note that the histograms in Figures 2Ci–iii peak at values which are out of the figure frame.

is evenly spread between the two modes of the stationary distribution (as in Figure 2Ai) than it is for the two gamma initial distributions (Figures 2Bi and 2Ci). This indicates that the transfer between the two peaks operates on a time-scale that is considerably slower than the unit time-scale of decay.

3 The toggle switch

By the toggle switch we mean a motif involving two mutually antagonistic genes. Toggle switches have been examined both by deterministic and various kinds of stochastic approaches. Even in the deterministic regime, there is a variety of different models, each following a specific set of assumptions on the interaction between the two antagonists. Here we focus on one that was previously used to model a synthetically engineered antagonism between LacI and cI [23], and also a switch between hematopoietic lineage determinants Gfi-1 and Egr [41]. The model is appropriate for a pair of genes which are governed by separate promoters, each being transcriptionally repressed by the cooperative action of the proteins encoded by the other gene [23]. Different descriptions follow if the genes are governed by a shared promoter [24], if either gene positively regulates itself [42], or if the antagonism is brought about by direct protein-protein interactions [43].

Stochastic models for gene switches are typically based on the discrete formulation of chemical kinetics [24, 26, 28, 44]. Alternatively, they may be obtained from a deterministic description by extending it by a phenomenological source of noise. For example, a system of differential equations representing the dynamics of a gene switch can first be discretised using the Euler method, which yields a system of difference equations, the right-hand sides of which can then be re-interpreted as random Poisson increments [25]. Superimposing a Gaussian noise term on a system of differential equations provides a similar means for turning a deterministic model into a stochastic one [29].

Hybrid stochastic descriptions of the toggle switch are also available [11, 27]. In [11], transcriptional repression decreases the duration of promoter activity period. In the bursting regime, this implies that repression leads to bursts of low size, rather than infrequent ones, which follow from the model examined below. Newby [27] considers (and analyses with matched asymptotics) the case of fast promoter transitions and slow protein synthesis/decay. Switch-like behaviour in hybrid models has been examined in a number of other contexts in mathematical biology, such as molecular transport [45] or spontaneous action potentials [46].

We consider two transcription factors X and Y with levels x and y, whose transcription is stochastic: TF X is transcribed with rate $a_1 = a_1(y)$ that functionally depends on

the level of TF Y; the transcription of Y occurs with rate $a_2 = a_2(x)$. Both functional dependencies are given by the Hill expressions

$$a_1(y) = \frac{r_1 K_1^m}{K_1^m + y^m}, \quad a_2(x) = \frac{r_2 K_2^n}{K_2^n + x^n},$$

where $m > 0$ and $n > 0$. Here r_1 and r_2 are the maximal transcription rates, while the dissociation constants K_1 and K_2 give the levels of Y and X necessary to reduce the transcription rate of the other by half. The transcription of the gene coding for X (Y) results in an increase in the amount of the factor by an exponentially distributed random quantity with mean b_1 (b_2). Both X and Y are degraded deterministically, with rate constants γ_1 and γ_2.

3.1 Burst times

If levels x of X and y of Y are observed at the initial time $t = 0$, then $x\mathrm{e}^{-\gamma_1 t}$ and $y\mathrm{e}^{-\gamma_2 t}$ give the levels of X and Y at a later time $t > 0$, given that no burst of either X or Y took place by then. The hazard function of the waiting time until the next transcription burst at either gene is given as the sum

$$h(t) = h_1(t) + h_2(t)$$

of individual hazard rates for bursts of X and those of Y, which are given by

$$h_1(t) = a_1(y\mathrm{e}^{-\gamma_2 t}) = \frac{r_1 K_1^m}{K_1^m + y^m \mathrm{e}^{-m\gamma_2 t}}, \quad h_2(t) = a_2(x\mathrm{e}^{-\gamma_1 t}) = \frac{r_2 K_2^n}{K_2^n + x^n \mathrm{e}^{-n\gamma_1 t}}.$$

The functional form of the above hazard rates is the same as that of the hazard function of a regulated transcription burst in the autoregulation model. This hazard function led to an explicit formula (11) for drawing a candidate waiting time for a regulated transcription burst. Analogously, for the present problem we find that we can draw candidate waiting times t_1 for a burst of X and t_2 for a burst of Y by setting

$$\begin{aligned} t_1 &= \frac{1}{m\gamma_2} \ln\left(u_1^{-\frac{m\gamma_2}{r_1}} \left(1 + (y/K_1)^m\right) - (y/K_1)^m \right), \\ t_2 &= \frac{1}{n\gamma_1} \ln\left(u_2^{-\frac{n\gamma_1}{r_2}} \left(1 + (x/K_2)^n\right) - (x/K_2)^n \right), \end{aligned} \tag{14}$$

where u_1 and u_2 are independent random variates drawn from the standardised uniform distribution. The waiting time t until the next burst occurs is the earlier of the two candidate waiting times,

$$t = \min(t_1, t_2).$$

Indeed, this random variate obeys the probability law defined by the total hazard function $h(t)$ due to Lemma 1.

Require: An initial distribution $(X^{(0)}, Y^{(0)}) \geq 0$ and a parameter set (r_1, r_2, K_1, K_2, m, n, b_1, b_2, γ_1, γ_2).

Return: A sample trajectory $(x(t), y(t))$, $t \geq 0$, of TF expression dynamics.

Draw the initial state $(x^{(0)}, y^{(0)})$ from the initial distribution $(X^{(0)}, Y^{(0)})$.
Set the current time and state: $t \leftarrow 0$; $x(0) \leftarrow x^{(0)}$; $y(0) \leftarrow y^{(0)}$.
loop
  Draw three independent random variates u_1, u_2 and $\tilde{u}$ from the standardised uniform distribution.
  Set $\tau_1 \leftarrow \frac{1}{m\gamma_2} \ln\left(u_1^{-\frac{m\gamma_2}{r_1}} \left(1 + (y(t)/K_1)^m\right) - (y(t)/K_1)^m \right)$.
  Set $\tau_2 \leftarrow \frac{1}{n\gamma_1} \ln\left(u_2^{-\frac{n\gamma_1}{r_2}} \left(1 + (x(t)/K_2)^n\right) - (x(t)/K_2)^n \right)$.
  Set $\tau \leftarrow \min\{\tau_1, \tau_2\}$.
  Set $x(t+\delta) \leftarrow x(t)\mathrm{e}^{-\gamma_1 \delta}$ for $0 < \delta < \tau$.
  Set $y(t+\delta) \leftarrow y(t)\mathrm{e}^{-\gamma_2 \delta}$ for $0 < \delta < \tau$.
  if $\tau = \tau_1$ **then**
    Set $x(t+\tau) \leftarrow x(t)\mathrm{e}^{-\gamma_1 \tau} - b_1 \ln(\tilde{u})$.
    Set $y(t+\tau) \leftarrow y(t)\mathrm{e}^{-\gamma_2 \tau}$.
  else
    Set $x(t+\tau) \leftarrow x(t)\mathrm{e}^{-\gamma_1 \tau}$.
    Set $y(t+\tau) \leftarrow y(t)\mathrm{e}^{-\gamma_2 \tau} - b_2 \ln(\tilde{u})$.
  end if
  Update the current time: $t \leftarrow t + \tau$.
end loop

Algorithm 2: Hybrid simulation of the toggle switch.

Immediately before the burst time t, the level of X is $x\mathrm{e}^{-\gamma_1 t}$ and the level of Y is $y\mathrm{e}^{-\gamma_2 t}$. If $t = t_1 < t_2$, then the burst was that of X, and the level of X is increased by an exponentially distributed amount with mean b_1, while the level of Y remains unchanged by the event. Therefore, by the inversion sampling method, the levels $\tilde{x}$ and $\tilde{y}$ of X and Y right after the burst are given by

$$\tilde{x} = x\mathrm{e}^{-\gamma_1 t} - b_1 \ln \tilde{u}, \quad \tilde{y} = y\mathrm{e}^{-\gamma_2 t} \quad \text{if } t = t_1 < t_2,$$

where $\tilde{u}$ is a random variate drawn from the standardised uniform distribution independently of u_1 and u_2. On the other hand, if $t = t_2 < t_1$, then the burst was that of Y, after which the levels are updated to

$$\tilde{x} = x\mathrm{e}^{-\gamma_1 t}, \quad \tilde{y} = y\mathrm{e}^{-\gamma_2 t} - b_2 \ln \tilde{u} \quad \text{if } t = t_2 < t_1,$$

where $\tilde{u}$ is, again, a random variate drawn from the standardised uniform distribution independently of u_1 and u_2. Thus, having started at time zero with the levels x and y, we are able to sample the dynamics of X and Y levels until the next burst occurs, at which point the levels are $\tilde{x}$ and $\tilde{y}$. Looping this procedure, we are able to determine the dynamics until any number of bursts occur, i.e. for a time interval of any pre-determined length. The resulting method is summarised in pseudocode as Algorithm 2.

3.2 Simulations

We examine the types of qualitative behaviour exhibited by the hybrid formulation of the toggle switch. We focus on the situation in which the two factors are assumed to have equivalent biological properties, i.e. we consider that the two transcription factors have a common degradation rate constant $\gamma_1 = \gamma_2 = \gamma$, maximal transcription rate $r_1 = r_2 = r$, dissociation constant $K_1 = K_2 = K$, Hill coefficient $m = n = \beta$ and mean amount $b_1 = b_2 = b$ of protein produced per transcription event. The number of parameters of the model can further be reduced by measuring time in units of the protein lifetime $1/\gamma$ and protein level in units of mean burst size b; these choices of units correspond to taking $\gamma = 1$ and $b = 1$. Therefore, to examine the qualitative behaviour of the toggle switch in the symmetric case, it is sufficient to consider the parameter sets of the form

$$\gamma_1 = \gamma_2 = 1, \quad r_1 = r_2 = r, \quad K_1 = K_2 = K, \quad m = n = \beta, \quad b_1 = b_2 = 1, \tag{15}$$

i.e. we need to explore only a three-dimensional parameter space $r \geq 0$, $K \geq 0$ and $\beta \geq 0$.

The deterministic formulation of the toggle switch model for the symmetric parameter set (15) is given by two ordinary differential equations

$$\frac{\mathrm{d}x}{\mathrm{d}t} = \frac{r}{1 + (y/K)^\beta} - x, \quad \frac{\mathrm{d}y}{\mathrm{d}t} = \frac{r}{1 + (x/K)^\beta} - y. \tag{16}$$

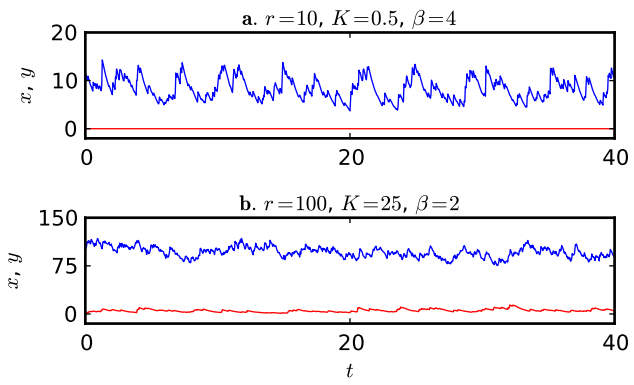

Figure 3: Trajectories of the toggle switch for chosen parameter sets.

This planar dynamical system is bistable, see [47], if

$$\beta > 1 \quad \text{and} \quad r/K > \beta(\beta-1)^{-1-1/\beta}; \tag{17}$$

the two stable steady states represent two possible biological states of the motif: one with the factor X switched on and the factor Y switched off ($X^{hi}Y^{lo}$) and the other state characterized by the reverse combination ($X^{lo}Y^{hi}$). If either of the above conditions for bistability of the planar system is not met, the system possesses a single stable steady state at which the two factors X and Y are coexpressed at equal levels.

In stochastic models such as one that we are currently studying, there always exists a unique stationary distribution, and therefore the initial condition has no effect on the state of the system in the limit of infinite time. Nevertheless, the hybrid toggle switch model can exhibit a metastable behaviour, which is practically tantamount to bistability: the transcription factors can be expressed either in a $X^{hi}Y^{lo}$ state or a $X^{lo}Y^{hi}$ state; transitions between these states occur on an extremely slow timescale so that the model can be considered practically bistable on a moderate timescale. For the toggle switch to exhibit metastable behaviour, it is necessary (but not sufficient) that the parameter values r, K and β satisfy the condition (17) for bistability of the deterministic model (16); as a rule of thumb, one can expect metastable behaviour of the stochastic model if the inequalities (17) are met by a sufficiently large margin.

The metastable scenario of the toggle switch is illustrated in two sample trajectories in Figures 3a–b that were generated using the hybrid Algorithm 2. In Figure 3a, we used the parameter values $r = 10$, $K = 0.5$, $\beta = 4$. The initial levels at $t = 0$ were set to $x = 10$ and $y = 0$, which correspond to having a high amount of the factor X (blue curve in the figure) and no factor Y (red curve) in the system at the initial time. We observe that the system remains in the state of high levels of X and lack of Y over a

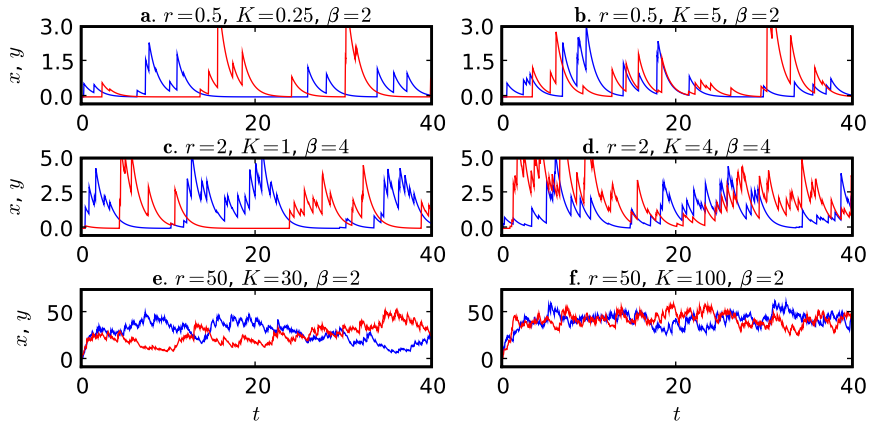

Figure 4: Trajectories of the toggle switch for chosen parameter values.

long period of time ($t < 40$).

Indeed, a very simple calculation shows that the transcription of Y is tightly repressed. From Figure 3a we see that the amount of the factor X fluctuates within the range 5 to 15. Using the lower bound, $x = 5$, we can estimate that at any given time the transcription propensity of Y is bounded above by $r/(1+(x/K)^{\beta}) \approx 10^{-3}$; therefore, we can expect that the factor Y will first be transcribed at a time t of order 10^3 or higher.

In Figure 3b we show a different kind of metastable behaviour of the stochastic model, in which both transcription factors are expressed simultaneously, albeit one of them at high and the other one at low levels. Stochastic simulations show that this kind of qualitative behaviour type can be observed only for high levels of the parameter r (in the example shown in the figure we chose $r = 100$, $K = 25$, $\beta = 2$).

In addition to the metastable scenarios, the hybrid model for the toggle switch exhibits a variety of distinct non-metastable sub-regimes, which are presented in Figures 4a–f. In Figure 4a we chose a parameter set ($r = 0.5$, $K = 0.25$, $\beta = 2$) for which the competition between the two antagonistic transcription factors is relatively strong, i.e. if X is expressed, then Y is repressed and vice versa. However, the low rate of transcription in this case causes the expression of either of these factors to be significantly stochastic, and the state of the system switches several times between the two biological states of the toggle switch within the temporal period $0 < t < 40$, thus forgetting the initial condition given at the time $t = 0$. The mutual exclusivity of the expression of the two factors can be modified by perturbing the dissociation constant K, which gives the threshold value for their mutual repression. In Figure 4b we show a sample path for a parameter set obtained from that of Figure 4a by increasing this threshold significantly to $K = 5$; the expression of the two factors is no longer exclusive. Yet another parameter set ($r = 2$,

$K = 1$, $\beta = 4$), bringing about the alternating exclusive expression pattern of the toggle switch motif, is shown in Figure 4c to illustrate the robustness of such behaviour; again, exclusivity in expression is lost if the value of K is increased to 4, as shown in Figure 4d.

All sample paths in Figures 4a–d are characterized by low values of the maximal transcription rate r, which makes the expression profiles of the transcription factor amounts intrinsically noisy. For high values of the parameter r, the non-metastable behaviour of the toggle switch is characterized by lesser noise and by the simultaneous expression of both factors, which is illustrated in Figures 4e, f. The parameter sets used for the sample paths in these two figures differ only in the value of threshold: if K is high, X and Y are coexpressed and are almost uncorrelated (cf. Figure 4f); for lower values of K, the amounts of the two factors become significantly negatively correlated (cf. Figure 4e). If we decrease the value of K further, we enter the metastable mode of the stochastic model (not shown but analogous to the metastable cases discussed above).

Thus, using the hybrid simulation Algorithm 2, we were able to classify the characteristic types of the toggle switch dynamics in the bursting regime of gene expression. In addition, large-scale simulations can be used to estimate the steady-state joint distribution of the levels of the antagonistic factors [40].

4 Discussion

In gene expression, proteins are produced in bursts of many copies, while they are degraded one molecule at a time. Consequently, protein production contributes to the overall gene-expression noise by a far larger share than the decay process. The hybrid modelling formalism based on this premise was applied in this paper to examine some relatively simple and fundamental regulatory motifs.

First, we characterised the statistics of transcription burst times in the autoregulatory loop motif. Like many other authors we used the Hill function to describe the autoregulation response curve. We found the hazard rate for a burst to occur to follow a relatively simple functional form. From this we derived the cumulative distribution function (10) for the waiting time until the burst occurs, and, by the inversion sampling method, found a means for drawing this waiting time (11). The method for drawing the waiting time is exact in the same sense as is the choice of the next reaction time in the classical Gillespie algorithm [48]: it does not introduce any numerical error except for that which is incurred by the evaluation of the closed-form expression (11).

The only further subtlety in the determination of the waiting time is due to leaky transcription, i.e. the expression at a low constant rate under a complete transcriptional

repression. In order to obtain the correct waiting time, we first determined the candidate waiting time for a leaky transcription (a simple exponential), then the candidate waiting time for the regulated transcription (as described above), taking the earlier of the two for the realised waiting time. The approach is analogous to the "first-reaction" implementation of the Gillespie algorithm [49].

Once the burst time is determined, the level of TF right after the burst is obtained by discounting the amount that was degraded during the time of waiting and then by including the new proteins synthesised in the burst. We may then look anew for the next burst time, and then for the one after that, etc., and in doing so we end up with the hybrid simulation Algorithm 1. The simulations of a positive autoregulation loop were shown to be in agreement with a previous analytic approach [19].

We extended the hybrid model for autoregulation to the toggle switch motif that involves two antagonistic transcription factors X and Y. In a hybrid formulation of the toggle switch, there are two distinct kinds of random events: bursts of the transcription of X and those of Y. The waiting time until the next burst occurs can be obtained by taking the minimum of the two candidate waiting times for either kind of bursts. The candidate waiting times follow a distribution of a form that has already been encountered in the autoregulation model and from which random variates can be sampled exactly. Which one occurs first determines whether it is X or Y whose transcription is realised. The levels of the factors immediately after the burst event are obtained first by discounting the amounts degraded during the time of waiting and then by including the new proteins of that species whose transcription was realised in the event. The specification of the next burst time and the determination of the resulting expression state are the basis for the hybrid toggle switch simulation algorithm (Algorithm 2).

The hybrid toggle switch model depends on eight dimensional and two dimensionless parameters; of the total ten parameters, six determine the Hill response curves, two give the deterministic degradation rate constants, and the remaining two are the mean burst sizes of X and Y. The parameter space was reduced by stipulating symmetry (15) in parameter values. Biologically, the symmetry constraint will be satisfied by an idealised pair of completely interchangeable transcription factors. Measuring time in the units of TF lifetime, and abundance in the units of mean burst size, leaves us with three dimensionless parameters only: r gives the average number of bursts per TF lifetime in the absence of repression; K gives the TF level (in the units of mean burst size) necessary to reduce the other's transcription rate by half; β is the Hill coefficient that determines the sharpness of the mutual repression between the factors.

The algorithm was used to characterise the various distinct qualitative types of behaviour that the toggle switch can exhibit under the symmetric constraint as the

three remaining dimensionless parameters r, K and β are varied. The first distinction was made between the metastable and non-metastable behaviour. The former occurs if $\beta > 1$ (high cooperativity) and r is substantially larger than K; the latter follows otherwise.

The metastable behaviour can further be subdivided into two categories. The first is characterised by a complete repression of one factor by the other (Figure 3a). The level of the highly expressed factor fluctuates widely, and a single transcription burst of the repressed factor can lead to a switch reversal. Only tight repression (requiring a low value of K) ensures that this happens very infrequently, as would typically be desirable of a biological switch [50].

The second kind of metastable behaviour, illustrated in Figure 3b requires a much higher value of r, resulting in smaller fluctuations of the highly expressed factor. The repressed factor can be transcribed at a background rate (unless K is very low); however, the consistently high levels of the antagonist make a spontaneous reversal of the switch highly improbable.

The metastable behaviour, of either sub-category, is a stochastic analogy of the bistable scenario of the deterministic reduction (16) of the toggle switch. Multistability in the deterministic and metastability in the stochastic model both imply that a single regulatory motif, specifically the toggle switch, can exhibit multiple distinct stable expression patterns. It is the cell's history, here the initial data, that specifies which one is selected.

The ability of a regulatory network to remember past choices is of a particular importance in the process of cellular development. Genetic switches, which can perform that role, are ubiquitous in genetic regulatory networks governing developmental processes [51]. The transcription factors X and Y of a toggle switch may act as lineage determinants, each activating a separate gene programme specific to a particular lineage. Mutual repression between the lineage determinants maintains the exclusivity of lineage commitment. Hybrid modelling enabled us to identify two distinct scenarios of how the repression may be realised in the presence of gene-expression noise.

The hybrid toggle switch exhibits a non-metastable behaviour if the initial conditions do not influence its expression dynamics at timescales that are significantly longer than the mean TF lifetime (here scaled to one). Metastability breaks down if there is too much noise (r is small), if the repression threshold is too high (K is large) or if the repression is not sufficiently cooperative (β not sufficiently larger than one).

The non-metastable behaviour is a stochastic counterpart to the mono-stable scenario of the deterministic formulation (16) of the toggle switch. In the monostable scenario, the deterministic model possesses a single stable steady state, which is situ-

ated on the diagonal $x = y$ when the symmetry constraint (15) holds. Such a stable steady state implies that, irrespective of the initial conditions, the expression of the two factors stabilises in time at equal levels.

The co-expression scenario has been used to explain the gene-expression profiles observed in stem and progenitor cells. Prior to committing itself to a particular lineage, a stem cell or a progenitor cell co-expresses genes affiliated to the various differentiated lineage programmes. The phenomenon, referred to as *multilineage priming* or *lineage promiscuity*, has been modelled by the co-expression scenario of the genetic switch between the lineage determinants [41].

The simulations of the hybrid toggle switch in the non-metastable regime provide two scenarios for the dynamics of multilineage priming in the presence of gene-expression noise. In the "fluctuating" scenario, at any single time point one of the factors is expressed and the other turned off (Figures 4a,c). The switching between the two available patterns is frequent owing to large noise levels. On the other hand, in the "simultaneous" scenario, both factors are expressed at any single time at relatively lower noise levels (e.g. Figure 4f). While in the fluctuating scenario the progenitor cell wavers between the two available programmes, in the simultaneous scenario it exhibits mixed lineage characteristics. We conclude that the relatively simple hybrid formulation of the toggle switch can account for the concepts of fluctuating and simultaneous multilineage priming [52]. We expect that qualitatively similar results would be obtained not only for our specific gene-switch model, but also for a broad range of plausible choices of switching mechanisms subject to bursting gene expression.

Hybrid modelling and simulation techniques applied in this paper to the autoregulation loop and the toggle switch motifs can be extended to investigate other motifs. The gene-regulation response functions can be of any suitable form previously suggested for deterministic models, such as those based on the Shea-Ackers formalism [53], or the Heaviside step function [54]. Transcription factors obeying hybrid dynamics can be combined in a single model with ones following a purely deterministic dynamics described by ordinary differential equations.

In such a general hybrid model, the distribution of the waiting time for the next burst will not follow a form as simple as that obtained for the examples studied in this paper; a more general — if less effective —procedure, based on rejection sampling, may then be applied. The exact simulation procedure can nevertheless be applied directly to an important special kind of motifs: those in which transcription factors regulate genes synergistically. In such motifs, the transcription rate of any individual gene is given by a sum of Hill response curves, or similar simple functions. For any pair T_1 and T_2 of transcription factors involved in the motif we may consider the candidate waiting

time of a burst of T_1 regulated by T_2. These candidate variables follow the distribution described in the analysis of the autoregulation loop, from which random variates can be sampled directly using the inversion method; the minimal candidate waiting time over all pairs gives the realised waiting time.

In summary, a hybrid modelling and simulation framework was applied in this paper to study the transcriptional dynamics of the autoregulation loop and of the toggle switch. For the former, we reported an agreement with previous analytic results, while the latter's behaviour was interpreted in the context of cell-fate selection. Other possible uses of the hybrid framework have also been discussed.

Acknowledgements

P. Bokes was supported by the European Commission under Marie Curie Early Stage Researcher Training (contract no. MEST-CT-2005-020723) and also by the Slovak Research and Development Agency (contract no. APVV-0134-10). J. King gratefully acknowledges the funding of the BBSRC/EPSRC (reference no. BB/D008522/1) and of the Royal Society and Wolfson Foundation.

References

[1] P. Lu, C. Vogel, R. Wang, X. Yao, and E.M. Marcotte. Absolute protein expression profiling estimates the relative contributions of transcriptional and translational regulation. *Nat. Biotechnol.*, 25:117–24, 2007.

[2] Y. Taniguchi, P.J. Choi, G.W. Li, H. Chen, M. Babu, J. Hearn, A. Emili, and X.S. Xie. Quantifying E. coli proteome and transcriptome with single-molecule sensitivity in single cells. *Science*, 329:533–8, 2010.

[3] D. Zenklusen, D.R. Larson, and R.H. Singer. Single-rna counting reveals alternative modes of gene expression in yeast. *Nat. Struct. Mol. Biol.*, 15:1263–1271, 2008.

[4] M.H.A. Davis. Piecewise-deterministic markov processes: A general class of non-diffusion stochastic models. *J. R. Stat. Soc. B*, 46:353–388, 1984.

[5] A. Singh and J.P. Hespanha. Stochastic hybrid systems for studying biochemical processes. *Philos. T. R. Soc. A*, 368:4995–5011, 2010.

[6] H.G. Othmer, S.R. Dunbar, and W. Alt. Models of dispersal in biological systems. *J. Math. Biol.*, 26(3):263–298, 1988.

[7] D.J. Bicout. Green's functions and first passage time distributions for dynamic instability of microtubules. *Phys. Rev. E*, 56(6):6656–6667, 1997.

[8] C.C. Chow and J.A. White. Spontaneous action potentials due to channel fluctuations. *Biophys. J.*, 71:3013–3021, 1996.

[9] T. Lipniacki, P. Paszek, A. Marciniak-Czochra, A.R. Brasier, and M. Kimmel. Transcriptional stochasticity in gene expression. *J. Theor. Biol.*, 238:348–67, 2006.

[10] A. Bobrowski, T. Lipniacki, K. Pichór, and R. Rudnicki. Asymptotic behavior of distributions of mrna and protein levels in a model of stochastic gene expression. *J. Math. Anal. Appl.*, 333:753–769, 2007.

[11] S. Zeiser, U. Franz, O. Wittich, and V. Liebscher. Simulation of genetic networks modelled by piecewise deterministic Markov processes. *IET Syst. Biol.*, 2:113–35, 2008.

[12] S. Zeiser, U. Franz, J. Müller, and V. Liebscher. Hybrid modeling of noise reduction by a negatively autoregulated system. *B. Math. Biol.*, 71:1006–1024, 2009.

[13] S. Zeiser, U. Franz, and V. Liebscher. Autocatalytic genetic networks modeled by piecewise-deterministic markov processes. *J. Math. Biol.*, 60:207–246, 2010.

[14] E. Cinquemani, R. Porreca, G. Ferrari-Trecate, and J. Lygeros. Subtilin production by bacillus subtilis: Stochastic hybrid models and parameter identification. *IEEE T. Automat. Contr.*, 53:38–50, 2008.

[15] A. Crudu, A. Debussche, and O. Radulescu. Hybrid stochastic simplifications for multiscale gene networks. *BMC Syst. Biol.*, 3:89, 2009.

[16] D.J. Higham, S. Intep, X. Mao, and L. Szpruch. Hybrid simulation of autoregulation within transcription and translation. *BIT*, 51:177–196, 2011.

[17] P. Bokes, J.R. King, A.T.A. Wood, and M. Loose. Multiscale stochastic modelling of gene expression. *J. Math. Biol.*, 2012.

[18] A. Raj, C.S. Peskin, D. Tranchina, D.Y. Vargas, and S. Tyagi. Stochastic mRNA synthesis in mammalian cells. *PLoS Biol.*, 4:e309, 2006.

[19] N. Friedman, L. Cai, and X.S. Xie. Linking stochastic dynamics to population distribution: an analytical framework of gene expression. *Phys. Rev. Lett.*, 97:168302, 2006.

[20] J. Lei, M.C. Mackey, R. Yvinec, and C. Zhuge. Adiabatic reduction of a piecewise deterministic markov model of stochastic gene expression with bursting transcription. *Arxiv preprint arXiv:1202.5411*.

[21] J.S. Griffith. Mathematics of cellular control processes. I. Negative feedback to one gene. *J. Theor. Biol.*, 20:202–8, 1968.

[22] J.S. Griffith. Mathematics of cellular control processes. II. Positive feedback to one gene. *J. Theor. Biol.*, 20:209–16, 1968.

[23] T.S. Gardner, C.R. Cantor, and J.J. Collins. Construction of a genetic toggle switch in Escherichia coli. *Nature*, 403:339–42, 2000.

[24] T.B. Kepler and T.C. Elston. Stochasticity in transcriptional regulation: origins, consequences, and mathematical representations. *Biophys. J.*, 81:3116–3136, 2001.

[25] T. Tian and K. Burrage. Stochastic models for regulatory networks of the genetic toggle switch. *P. Natl. Acad. Sci. USA*, 103:8372–8377, 2006.

[26] A. Loinger, A. Lipshtat, N.Q. Balaban, and O. Biham. Stochastic simulations of genetic switch systems. *Phys. Rev. E*, 75:021904, 2007.

[27] J.M. Newby. Isolating intrinsic noise sources in a stochastic genetic switch. *Arxiv preprint arXiv:1111.1415*.

[28] B. Munsky and M. Khammash. Identification from stochastic cell-to-cell variation: a genetic switch case study. *IET Syst. Biol.*, 4:356–366, 2010.

[29] M. Andrecut, J.D. Halley, D.A. Winkler, and S. Huang. A general model for binary cell fate decision gene circuits with degeneracy: Indeterminacy and switch behavior in the absence of cooperativity. *PloS one*, 6:e19358, 2011.

[30] J.D. Murray. *Mathematical Biology*. Springer, 2003.

[31] J. Keener and J. Sneyd. *Mathematical Physiology: Cellular Physiology*. Springer, 2008.

[32] U. Alon. *An Introduction to Systems Biology: Design Principles of Biological Circuits*. Chapman & Hall/CRC, 2007.

[33] M.C. Mackey, M. Tyran-Kaminska, and R. Yvinec. Molecular distributions in gene regulatory dynamics. *J. Theor. Biol.*, 274:84–96, 2011.

[34] M.C. Mackey and M. Tyran-Kaminska. Dynamics and density evolution in piecewise deterministic growth processes. *Ann. Polon. Math.*, 94:111–129, 2008.

[35] N.G. van Kampen. *Stochastic Processes in Physics and Chemistry*. Elsevier, 2006.

[36] J.J. Tyson, K.C. Chen, and B. Novak. Sniffers, buzzers, toggles and blinkers: dynamics of regulatory and signaling pathways in the cell. *Curr. Opin. Cell Biol.*, 15:221–31, 2003.

[37] B. Novák and J.J. Tyson. Design principles of biochemical oscillators. *Nat. Rev. Mol. Cell Biol.*, 9(12):981–991, 2008.

[38] D.R. Cox and D. Oakes. *Analysis of Survival Data*. Chapman & Hall/CRC, 1984.

[39] C.P. Robert and G. Casella. *Monte Carlo Statistical Methods*. Springer, 2004.

[40] P. Bokes. *Genetic regulatory networks*. PhD thesis, University of Nottingham, 2010.

[41] P. Laslo, C.J. Spooner, A. Warmflash, D.W. Lancki, H.J. Lee, R. Sciammas, B.N. Gantner, A.R. Dinner, and H. Singh. Multilineage Transcriptional Priming and Determination of Alternate Hematopoietic Cell Fates. *Cell*, 126:755–766, 2006.

[42] S. Huang, Y.P. Guo, G. May, and T. Enver. Bifurcation dynamics in lineage-commitment in bipotent progenitor cells. *Dev. Biol.*, 305:695–713, 2007.

[43] P. Bokes, J.R. King, and M. Loose. A bistable genetic switch which does not require high co-operativity at the promoter: a two-timescale model for the PU. 1–GATA-1 interaction. *Math. Med. Biol.*, 26:117–32, 2009.

[44] M. Andrecut and S.A. Kauffman. Noise in genetic toggle switch models. *J. Int. Bioinform*, 23, 2006.

[45] J. Newby and P.C. Bressloff. Local synaptic signaling enhances the stochastic transport of motor-driven cargo in neurons. *Phys. Biol.*, 7:036004, 2010.

[46] J.P. Keener and J.M. Newby. Perturbation analysis of spontaneous action potential initiation by stochastic ion channels. *Phys. Rev. E*, 84:011918, 2011.

[47] J.L. Cherry and F.R. Adler. How to make a biological switch. *J. Theor. Biol.*, 203:117–33, 2000.

[48] D.T. Gillespie. Exact stochastic simulation of coupled chemical reactions. *J. Phys. Chem.*, 81:2340–61, 1977.

[49] D.T. Gillespie. A General method for numerically simulating stochastic time evolution of coupled chemical reactions. *J. Comput. Phys.*, 22:403–34, 1976.

[50] H.H. Chang, M. Hemberg, M. Barahona, D.E. Ingber, and S. Huang. Transcriptome-wide noise controls lineage choice in mammalian progenitor cells. *Nature*, 453:544–547, 2008.

[51] G. Swiers, R. Patient, and M. Loose. Genetic regulatory networks programming hematopoietic stem cells and erythroid lineage specification. *Dev. Biol.*, 294:525–40, 2006.

[52] M. Hu, D. Krause, M. Greaves, S. Sharkis, M. Dexter, C. Heyworth, and T. Enver. Multilineage gene expression precedes commitment in the hemopoietic system. *Genes Dev.*, 11:774–85, 1997.

[53] M.A. Shea and G.K. Ackers. The OR control system of bacteriophage lambda. A physical-chemical model for gene regulation. *J. Mol. Biol.*, 181:211–30, 1985.

[54] H. De Jong. Modeling and simulation of genetic regulatory systems: a literature review. *J. Comput. Biol.*, 9:67–103, 2002.